Relative Production of the $\chi_{c1}(1P)$ and $\chi_{c2}(1P)$

The CDF Collaboration
July 26, 2006

Abstract

The charmonium states χ_{c1} and χ_{c2} are reconstructed from their decays into J/$\psi\gamma$. The final state photon is reconstructed through conversion into electron-positron pairs, which gives a mass resolution sufficient for resolving these states. The technique is used to provide a measurement of the ratio of cross sections $\frac{\sigma_{\chi_{c2}}}{\sigma_{\chi_{c1}}} = 0.64 \pm 0.03(stat.) \pm 0.04(sys.) \pm 0.06(B.F.)$ for events with P_T(J/ψ) in the range 4-20 GeV/c. Information on the displacement of the final states from the beamline is used to separate the production mechanisms, and the cross section ratio from prompt production is found to be $\frac{\sigma_{\chi_{c2}}}{\sigma_{\chi_{c1}}} = 0.70{\pm}0.04(stat.){\pm}0.04(sys.){\pm}0.06(B.F.)$. The fraction of events attributable to B decay provide a measurement of $\frac{\sigma_B * B(B\to\chi_{c2})}{\sigma_B * B(B\to\chi_{c1})} = 0.25{\pm}0.07(stat.){\pm}0.01(sys.){\pm}0.02(B.F.)$. No significant variation in this quantity has been observed over the transverse momentum range studied. Furthermore, no significant production of χ_{c0} has been observed in this data.

1 Introduction

The study of charmonium production in hadronic collisions is now a fairly old industry. A long list of experiments, both fixed target and colliding beam, have contributed to this subject [1, 2]. Recent results from CDF on charmonium production include a measurement of the total χ_{cJ} contribution to J/ψ production [3], the relative ratio of $\chi_{c1}(1P)$ to $\chi_{c2}(1P)$ production [4] and the total J/ψ cross section [5]. The work in this note extends the Run 1 χ_{cJ} measurement by exploiting the new, larger data set that is now available.

Most models for hadronic J/ψ production predict a large component due to radiative decay from the P wave states, the χ_{cJ}'s. This is due to the fact that P wave charmonium can be produced through a two gluon process, while direct J/ψ production must involve three or more. Unfortunately, the radiative decay process $\chi_{cJ} \to J\psi\gamma$ is very difficult to measure due to the relatively low energy photon in this decay (303-430 MeV in the center of mass). Experiments that base their photon detection and measurement on calorimetric techniques generally lack the mass resolution to separate the contributions from the different spin states.

These experiments also tend to suffer from large backgrounds, due to other mechanisms for soft photon production in hadron collisions ($\pi^0 \to \gamma\gamma$, etc.). An alternative technique of photon reconstruction through conversion into electron pairs has been used by some groups to resolve the mass states. This method typically has superior mass resolution compared to calorimetric measurements, because most experiments operate in a region of phase space where their tracking systems provide greater momentum accuracy than their calorimeters for photons in this decay. However, the conversion technique generally has a low efficiency, so the measurements suffer from a small sample size and are statistically limited. The most precise measurements of $\frac{\sigma_{\chi_{c2}}}{\sigma_{\chi_{c1}}}$ for three different interactions environments are listed in Table I, and demonstrate this point. The small samples available with sufficient mass resolution to discern the two states result in large statistical uncertainties.

Table I: Prior measurements of the ratio of cross sections between the χ_{c1} and χ_{c2}

Interaction	$\sqrt{s}$(GeV)	$\frac{\sigma_{\chi_{c2}}}{\sigma_{\chi_{c1}}}$	Reference
$\pi^- -$ Be	29	$1.75 \pm 0.55(stat.) \pm 0.18(sys.)$	[6]
$p -$ Si	38	$1.88 \pm 0.71(stat.) \pm 0.25(sys.)$	[7]
$p - \overline{p}$	1800	$0.96 \pm 0.27(stat.) \pm 0.11(sys.)$	[4]

In this analysis, we will measure the ratio of cross sections between the two most plentiful χ_{cJ} states. This ratio will provide guidance for any theory of hadronic charmonium production. Some versions of the Color Evaporation Model predict a value of 5/3 for this ratio [2], but the prior measurements are too imprecise to provide much guidance. The data sample presented here will provide a new level of precision for this measurement.

2 Data Set and Method of Reconstruction

The data used for this measurement include all events recorded from April 2001 through Feb. 2006 at the Tevatron, and corresponds to 1.1 fb^{-1} of integrated luminosity. In this analysis, we reconstruct the final state $\chi_{cJ} \to J/\psi\gamma$, $J/\psi \to \mu^+\mu^-$ with the standard CDF trigger and selection. The photon is reconstructed through conversion into e^+e^- pairs, primarily occuring in the silicon detector system. The momentum resolution of the CDT drift chamber provides excellent invariant mass resolution, which allows the χ_{cJ} states to be unambiguously resolved. Furthermore, the precision position meassurement provided by the silicon vertex detector allows a clean separation between prompt χ_{cJ} production and production that has occured through the decay of B hadrons.

The following requirements are imposed on J/$\psi\gamma$ combinations to isolate a χ_{cJ} sample:

- The vertex constrained $\mu^+\mu^-$ mass must fall within 80 MeV/c^2 of the world average value [8].
- The probability of the complete J/$\psi\gamma$ constrained fit must exceed 10^{-5}.

- P_T(J/ψ) > 4.0 Gev/c.
- $P_T(\gamma)$ > 1.0 Gev/c.
- $abs(\eta$(J/ψ)) < 1.0.
- Radial position of the γ conversion > 12 cm from the beam.

The invariant mass spectrum of J/$\psi\gamma$ combinations are shown in Fig 1. Clearly separated signals can be seen for the χ_{c1} and χ_{c2}.

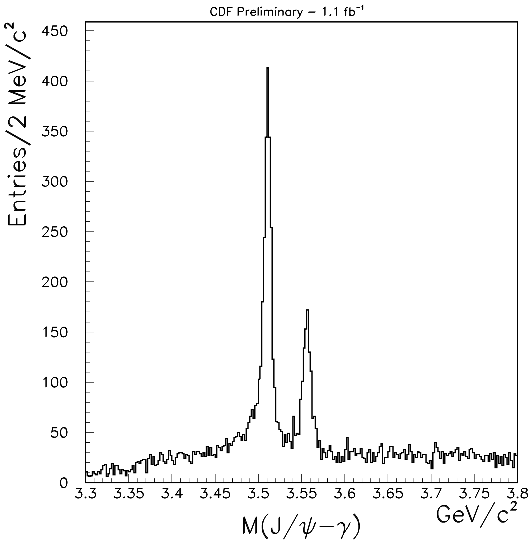

Figure 1: a. The J/$\psi\gamma$ mass distribution for all events used in the cross section ratio analysis.

3 Event Simulation

Reconstruction efficiency and acceptance of the χ_{cJ} states were studied with simulated events. The Monte Carlo used to understand our acceptance and resolution generated χ_{c1} and χ_{c2} in equal rates, the processed through the full trigger and detector simulations. Simulated signals appear in Fig. 2, along with the parametrization used to fit the measured mass spectrum.

Separation of the prompt and B decay contributions to the χ_{cJ} yield was obtained by an unbinned likelihood fit, which simultanaeously fits both mass and effective decay length. This effective decay length is parametrized as a function of $P_T(J/\psi)$ and has been used in earlier CDF analyses of χ_{cJ} production [3]. The full probability distribution function for the signal events is given for each event by

$$L(m^i, \lambda^i_{eff}) = ((1 - f_b) * L_{Prompt}(\lambda^i_{eff}) * L_{Prompt}(m^i) + f_b * L_B(\lambda^i_{eff}) * L_B(m^i), \tag{1}$$

where f_b is the fraction of events from B decay, λ_{eff} is the effective decay length, m^i is the invariant mass, and L_B, L_{prompt} are the mass distributions for B and prompt events respectively.

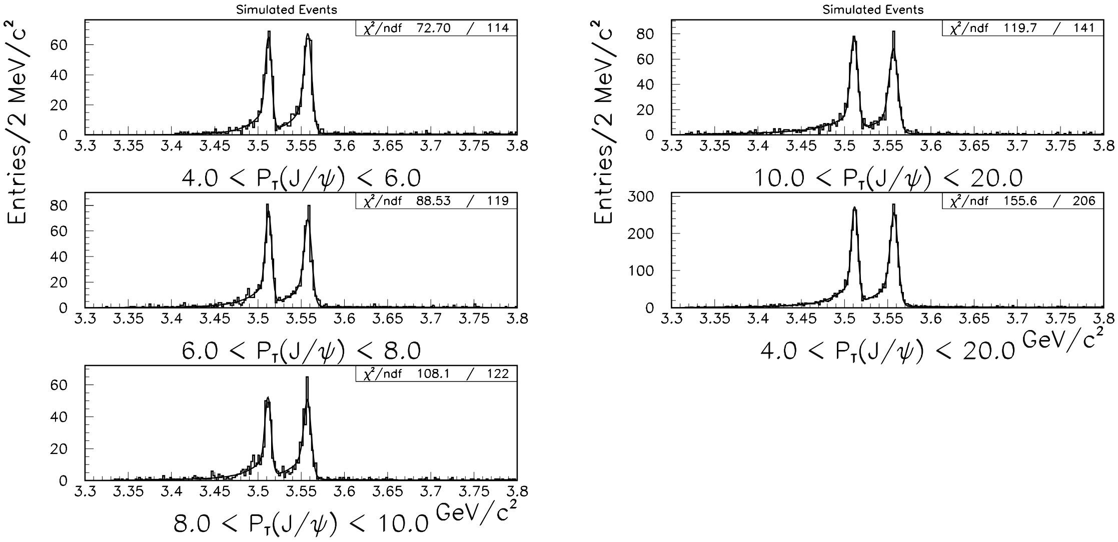

Figure 2: The J/$\psi\gamma$ invariant mass distribution from simulated events, for several ranges of $P_T(\mathrm{J}/\psi)$.

Polynomial terms are added for the background shapes used in the full fit to the data. The data, overlaid with projections of this likelihood function are shown in Fig. 3 The event yields obtained are listed in Table II.

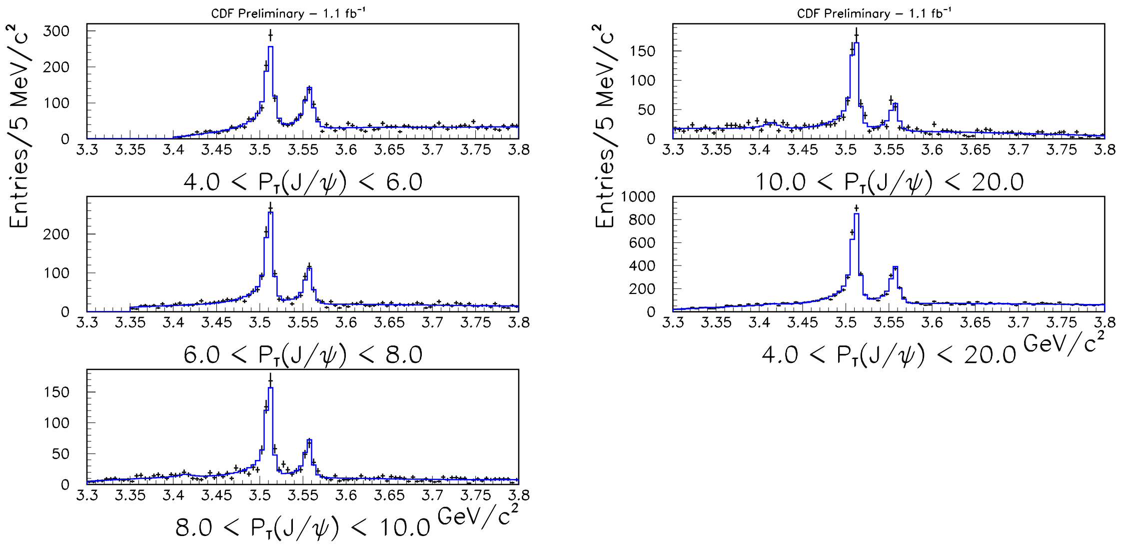

Figure 3: A comparison between the data and a projection of the unbinned likelihood function. In these plots, the mass spectrum is shown for all values of λ_{eff}. The projected fit is overlaid in blue.

Table II: Event yields calculated from fitting the data

$P_T(\mathrm{J}/\psi)$ (Gev/c)		Total	Prompt Events	B Decay
4-6	χ_{c0}	0±0.1	0.0±0.1	0.0±0.1
	χ_{c1}	793±34	697±32	96±9
	χ_{c2}	428±26	413±25	15±8
	$\frac{\chi_{c0}}{\chi_{c1}}$	-	-	-
	$\frac{\chi_{c2}}{\chi_{c1}}$	0.54±0.04	0.59±0.05	0.16±0.10
6-8	χ_{c0}	3±10	3±10	0.0±0.1
	χ_{c1}	755±36	676±33	79±16
	χ_{c2}	312±22	304±21	8±8
	$\frac{\chi_{c0}}{\chi_{c1}}$	0.0±0.01	0.0±0.01	0.0±0.01
	$\frac{\chi_{c2}}{\chi_{c1}}$	0.41±0.04	0.45±0.04	0.10±0.11
8-10	χ_{c0}	29±12	10±9	19±8
	χ_{c1}	454±30	355±25	99±16
	χ_{c2}	198±18	184±17	14±7
	$\frac{\chi_{c0}}{\chi_{c1}}$	0.07±0.03	0.03±0.03	0.18±0.09
	$\frac{\chi_{c2}}{\chi_{c1}}$	0.44±0.05	0.52±0.06	0.14±0.08
10-20	χ_{c0}	63±15	44±12	19±10
	χ_{c1}	527±33	420±28	107±18
	χ_{c2}	166±17	143±15	23±8
	$\frac{\chi_{c0}}{\chi_{c1}}$	0.11±0.03	0.10±0.03	0.16±0.10
	$\frac{\chi_{c2}}{\chi_{c1}}$	0.32±0.04	0.34±0.04	0.21±0.09
4-20	χ_{c0}	68±25	40±20	28±16
	χ_{c1}	2526±69	2141±60	385±35
	χ_{c2}	1104±43	1039±40	66±16
	$\frac{\chi_{c0}}{\chi_{c1}}$	0.03±0.01	0.02±0.01	0.07±0.04
	$\frac{\chi_{c2}}{\chi_{c1}}$	0.44±0.02	0.485±0.023	0.17±0.05

Table III: Relative Acceptances for the χ_{cJ} states

P_T(J/ψ)	$\frac{\alpha_{\gamma_2}}{\alpha_{\gamma_1}}$
4-6	1.271 $\pm$ 0.036
6-8	1.169 $\pm$ 0.028
8-10	1.139 $\pm$ 0.033
10-20	1.101 $\pm$ 0.043
4-20	1.226 $\pm$ 0.034

The uncertainties given in Table III reflect the statistical uncertainties due to the sample used in the simulation, and the statistical uncertainty on the cross section [5].

4 Results

The event yields given in Table II can now be combined with the relative acceptance ratios in Table III and the world average branching ratios [8] to give the relative cross sections between the χ_{cJ} states. A summary of the relavant properties of the χ_{cJ} states is given in Table IV. These

Table IV: Properties of the χ_{cJ} states [8]

	Mass (MeV/c^2)	Width (MeV/c^2)	$B(\chi_{cJ} \to J/\psi\gamma)$(%)
χ_{c0}	3415.16±0.35	10.2±0.8	1.13±0.11
χ_{c1}	3510.59±0.10	0.96±0.12	31.6±2.3
χ_{c2}	3556.26±0.11	2.25±0.15	17.8±0.8

results are given in Table V. The uncertainties given in Table V include only the statistical

Table V: Ratio of cross sections between the χ_{cJ} states

P_T(J/ψ)	$\frac{\sigma_{\chi_{c2}}}{\sigma_{\chi_{c1}}}$		
(Gev/c)	Total	Prompt Events	B Decay
4-6	0.768±0.073	0.810±0.073	0.349±0.168
6-8	0.607±0.062	0.683±0.063	0.061±0.152
8-10	0.670±0.080	0.810±0.096	0.218±0.125
10-20	0.500±0.067	0.548±0.068	0.322±0.146
4-20	0.637±0.034	0.702±0.040	0.246±0.073

uncertainties obtained from the fits to the data. Two additional uncertainties must be included in this calculation. The first will represent the systematic uncertainty on this analysis. The second will be due to the uncertainties on the branching ratios of the χ_{cJ} states into J/$\psi\gamma$. This second uncertainty is outside of our control, and will therefore be explicitly noted.

5 Systematic Uncertainties on $\frac{\sigma_{\chi_{c0,2}}}{\sigma_{\chi_{c1}}}$

5.1 Systematic Uncertainties on $\frac{N_{\chi_{c0,2}}}{N_{\chi_{c1}}}$

5.1.1 Fixing Radiative Tail Parameters

For the likelihood fits to the data, the signal shapes are assumed to be well characterized by the simulated events. In particular, the radiative tail shape is taken from the simulation and used for the data fit. The fits for each P_T range were repeated for variations of $\pm 1\sigma$ for each of the parameters used to define the mass distribution. When each parameter was varied, the other was also changed by a value determined by the correlation obtained between them The average change in the ratio of yield, $\frac{N_{\chi_{c2}}}{N_{\chi_{c1}}}$, was $\pm$ 0.005 for these $\pm 1\sigma$ parameter variations, so this will be taken as the systematic uncertainty for the radiative tail description.

5.1.2 Prompt/B Decay Separation

The definition of effective flight distance used for separation of the prompt and B decay components was taken from the Run I analysis which used the calorimeter to calculate the fraction of J/ψ production due to χ_{cJ} decay [3]. The sensitivity of the results to this assumption was tested by repeating the fit to the full J/$\psi\gamma$ sample for variations in the constants used in the λ_{eff} definition, as well as trivializing this parameterization to make the $P_T(B) = P_T(J\psi)$. A variation of ± 0.002 in the B decay fraction was found by varying this parametrization, which corresponds to a relative uncertainty of ± 0.007 in the yield ratio of the prompt sample. Similarly, a relative uncertainty of ± 0.01 is found for the B decay sample.

5.1.3 h_c Contribution to the Background

The inclusion of a possible background due to $h_c \to J\psi\pi^0$ was considered by simulating this process in our detector simulation, and repeating the signal fits with this added mass spectrum component. Our fits preferred a vanishingly small contribution to this process. Consequently, we will not quote a systematic uncertainty based on the existance, or branching fraction of the h_c.

5.2 Systematic Uncertainties on $\frac{\alpha_{\gamma_{0,2}}}{\alpha_{\gamma_1}}$

5.2.1 Uncertainty due to the Simulation Sample Size

The statistical uncertainty on the simulated sample is listed in Table III. This corresponds to a relative systematic uncertainty of 2.8% on the ratio of acceptances between the χ_{c1} and χ_{c2} for the full sample.

5.2.2 Photon Conversion Simulation

Two approaches to the consersion simulation have been studied. The first was a direct detector simulation. The second involved a parametrization of the final state electrons, and allowed a larger sample to be studied. Differences between the two suggested that a 2% systematic uncertainty was appropriate for the effect of the consversion simulation.

5.2.3 Polarization of the χ_{cJ} states

The acceptance calcualtion used in this analysis makes an inherent assumption that the J/ψ produced from each χ_{cJ} has the same likelihood of triggering the experiment and being reconstructed. This could break down if the mechanism of production were such that the polarization of the χ_{c1} were significantly different from that of the χ_{c2}. Polarization would affect the angular distribution of the muons from the J/ψ decay, and would result in an distribution of the form

$$I(\theta_{\mu\mu}) \propto 1 + \alpha * \cos^2(\theta_{\mu\mu}) \quad (2)$$

where $\theta_{\mu\mu}$ is the angle between the μ^+ and the J/ψ direction in the J/ψ rest frame, and α is a constant. This analysis will adopt the strategy used by the J/ψ cross section analysis [5], and use a value of $\alpha = 0.13 \pm 0.15$ for the spin alignment constant. Variation of the angular distribution for one of the χ_{cJ} states by ± 0.15 produced a $\pm 3\%$ variation was observed for the number of events that pass our muon selection at $P_T(J/\psi) = 4$ Gev. Consequently, we will adopt a 3% systematic uncertainty due to possibly different polarizations between the χ_{cJ} states.

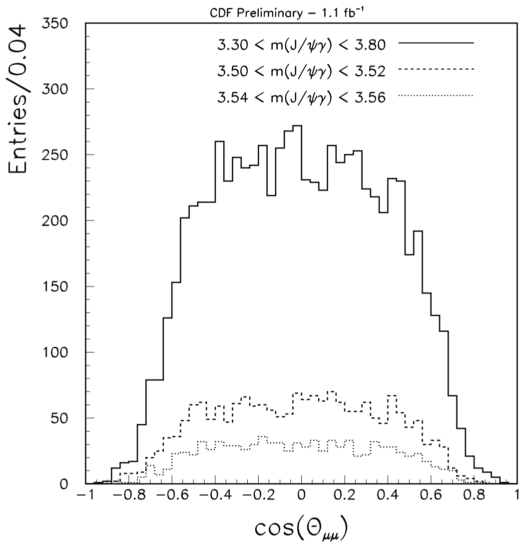

Figure 4: The $\cos(\theta_{\mu\mu})$ distribution for prompt events, for several ranges of J/$\psi\gamma$ invariant mass.

It should be noted that CDF has very poor sensitivity to the angular distribution parameter α in Eq. 2. This can be seen in Fig. 4, where $\cos(\theta_{\mu\mu})$ is plotted for all the data with

$|\lambda_{eff}| < 100\mu$m. This subsample will be predominantly prompt events. It is clear from Fig. 4, that very little data is available at high values of $|\cos(\theta_{\mu\mu})|$, where the sensivity would be greatest. This is due to the trigger, which requires a minimum transverse momentum of 1.5-2.0 Gev/c for each muon.

5.3 Systematic Uncertainties on $\frac{B(\chi_{c0,2}\to J/\psi\gamma)}{B(\chi_{c1}\to J/\psi\gamma)}$

The branching fraction uncertainties used in this analysis are simply taken from the Particle Data Group [8]. This experiment has no ability to improve upon them, so this uncertainty will simply be taken as the uncorrelated uncertainty of the individual branching fractions. Consequently, we will have a relative systematic uncertainty of 9% on $\frac{B(\chi_{c2}\to J/\psi\gamma)}{B(\chi_{c1}\to J/\psi\gamma)}$.

5.4 Total Systematic Uncertainties on $\frac{\sigma_{\chi_{c0,2}}}{\sigma_{\chi_{c1}}}$

To obtain the systematic uncertainty on $\frac{\sigma_{\chi_{c0,2}}}{\sigma_{\chi_{c1}}}$, we will treat the previously mentioned affects as uncorrelated uncertainties, and combine them in quadrature for an estimate of the total. The effects are summarized in Table VI. The total relative systematic uncertainty on the ratio

Table VI: Systematic Uncertainties

Affect	Relative Uncertainty	
	Prompt Events	B Decay Events
Radiative tail parameters	0.005	0.005
Prompt/B Separation	0.0015	0.01
h_c Background	0	0
Simulated Sample Size	0.028	0.028
Photon Simulation Strategy	0.02	0.02
Polarization Differences	0.03	0.03
Total	0.046	0.047

of cross sections attributable to this analysis is 0.046 and 0.047 for the prompt and B decay samples respectively. The branching fraction uncertainty is outside our control, and will be stated explicitly.

6 Summary and Conclusions

We have used the the CDF tracking and muon systems to reconstruct $\chi_{cJ} \to J/\psi\gamma$. The momentum resolution of the tracking system provides a mass resolution that is sufficient to clearly distinguish the three χ_{cJ} states and measure their relative contributions to J/ψ production. Furthermore, the position resolution of the tracking system makes it possible to separate prompt production from B decay contributions. For events in the kinematic range

$4.0 < P_T(\mathrm{J}/\psi) < 20.0$, $|\eta| < 1.0$, we find that $\frac{\sigma_{\chi_{c2}}}{\sigma_{\chi_{c1}}} = 0.64 \pm 0.03(stat.) \pm 0.04(sys.) \pm 0.06(B.F.)$ for all events, and $\frac{\sigma_{\chi_{c2}}}{\sigma_{\chi_{c1}}} = 0.70 \pm 0.04(stat.) \pm 0.04(sys.) \pm 0.06(B.F.)$ for events that are promptly produced. The fraction of events attributable to B decay provide a measurement of $\frac{\sigma_B * B(B \to \chi_{c2})}{\sigma_B * B(B \to \chi_{c1})} = 0.25 \pm 0.07(stat.) \pm 0.01(sys.) \pm 0.02(B.F.)$.

For convenient comparison to other authors, the prompt production result can be restated as $\frac{\sigma_{\chi_{c1}}}{\sigma_{\chi_{c2}}} = 1.43 \pm 0.08(stat.) \pm 0.07(sys.) \pm 0.13(B.F.)$ No statistically significant contribution to J/ψ production from the χ_{c0} has been observed. The data has been divided into smaller ranges of $P_T(\mathrm{J}/\psi)$. No clear behavior is indicated over the range studied.

References

[1] G. Schuler, Report No. CERN-TH/95-75

[2] N. Brambilla, *et. al.*, FERMILAB-FN-0779, CERN-2005-005, hep-ph/0412158.

[3] F. Abe, *et. al.*, Phys. Rev. Lett. **79**, 578 (1997)

[4] T. Affolder, *et. al.*, Phys. Rev. Lett. **86**, 3963 (2001)

[5] D. Acosta *et. al.*, Phys. Rev. **D71**, 032001 (2005).

[6] Koreshev, *et. al.*, Phys. Rev. Lett. **77**, 4294 (1996)

[7] Alexopoulos, *et. al.*, Phys. Rev. **D62**, 32006 (2000)

[8] Review of Particle Physics, S. Eidelman *et. al.*, Phys. Lett. B**592**, 1 (2004), and the 2005 partial update for the 2006 edition available on http://pdg.lbl.gov

[9] T. Affolder *et. al.*, Phys. Rev. Lett. **85**, 2886 (2000).